Spread-spectrum Multi-carrier Communication in Interference-limited Acoustic Regimes

Zhengnan Li, *Graduate Student Member, IEEE,* and Milica Stojanovic, *Fellow, IEEE*
Northeastern University, Boston, MA, USA

***Abstract*—Interference-limited regimes occur in underwater acoustic communication scenarios for a variety of reasons: (i) ambient noise levels can be elevated in certain environments, (ii) intentional interference can be present in adversarial situations, (iii) the signal level can be reduced deliberately so as to achieve security, and (iv) multi-user interference can be present in networked systems. We focus here on signal detection in low SNR regimes using multi-carrier modulation in the form of orthogonal frequency division multiplexing (OFDM). We propose a transmission / detection method that integrates OFDM with direct-sequence spectrum spreading. Specifically, we capitalize on coupling the channel estimation / signal detection with structured coding to obtain an efficient receiver design. We consider both coherent and differentially coherent detection, and extend the detection principles to multi-channel receiver configurations. In addition, spread-spectrum OFDM detection is coupled with a custom-designed frequency synchronization techniques to counteract the motion-induced Doppler frequency shifting. Using experimental recordings from the Mobile Acoustic Communication Experiment (MACE'10), where signals were transmitted over a 3 km – 7 km shallow-water channel in the 10.5 kHz – 15.5 kHz band, with relative transmitter / receiver motion of up to 1.5 m/s, we study the system performance in terms of the mean squared error and symbol error rate in data detection. Varying the level of externally added noise, we show that the proposed methods provide excellent performance while maintaining simplicity needed for a practical implementation.**

***Index Terms*—Underwater acoustic communication, low SNR, interference, multi-user communication, OFDM, direct sequence spread spectrum, channel estimation, differentially coherent detection, Doppler effect, frequency synchronization.**

I. Introduction

We address the design of an underwater acoustic communication system capable of operating in noisy or interference-limited regimes. Such regimes occur in different situations, which can roughly be classified as having unintentional or intentional interference. While unintentional interference is created by environmental sources, intentional interference occurs in hostile environments or in multi-user systems where other users of the same network operate simultaneously in the same frequency band. Additionally, in systems that require low probability of intercept (LPI), signal level is deliberately reduced so as to hide the signal below the noise, thus making it inaudible to an unintended listener.

Communication in an interference-limited regime is typically established using spread spectrum methods, either of the frequency hopping (FH) or the direct sequence (DS) type. Both types have been extensively studied for use in terrestrial and satellite systems. A well known example is the 3G cellular standard based on DS code-division multiple access (CDMA). DS spread spectrum with single-carrier modulation has also been studied for underwater acoustic communications [1], where the major difference from terrestrial radio communications was found to be in the channel's time-variability that required re-thinking of the basic despreading operation, and resulted in the concept of chip-rate hypothesis-feedback equalization. Further studies of single-carrier DS acoustic systems included e.g. [2], [3] and [4], where the focus was on strategic design of the DS spreading process to alleviate the multiapth problem in low SNR regimes. A less conventional approach to covert underwater acoustic communications was taken in [5], where information signals were embedded into recorded dolphin sounds for subsequent transmission over an acoustic channel.

An alternative to single-carrier broadband modulation is the multi-carrier modulation, typically implemented in the form of orthogonal frequency division multiplexing (OFDM). The attendant signal processing issues that address equalization and motion-induced frequency shifting in an acoustic channel have been well understood at this point; see e.g. [8], [9], [10]. The major advantages of OFDM are bandwidth scalability and FFT-based signal processing; the latter leading to computationally-simple receiver architectures if the system is kept free of inter-carrier interference (ICI). In light of covert communications, the advantage of OFDM is in the fact that the signal waveforms exhibit Gaussian-like characteristics in the time domain, thus making them noise-like provided that the signal level is kept low.

Coupling of OFDM and DS spread spectrum has been investigated in the mainstream radio literature (e.g. [6]),but references specific to underwater acoustic communications remain scarce. A notable exception is [7], where a time-frequency spreading method was proposed and evaluated using experimental data. The method is based on a multi-band OFDM approach, where the total available bandwidth is divided into several subbands, and each subband devoted to one OFDM stream (e.g. 16 subbands with 256 carriers each). A coded signal is repeated (spread) over the subbands, as well as over blocks in time. Coherent detection is employed, with pilots allocated to each subband at an overhead rate of about 50%. Channel estimation utilizes a basis expansion method, while equalization and despreading are performed jointly. Good performance is obtained at the expense of computationally-heavy signal processing.

In this paper, we propose a method for DS OFDM, which aims for computationally efficient processing at the receiver. The method is suitable for both low SNR and multi-user regimes, and allows for coherent, as well as differentially coherent detection. The latter is associated with very low computational complexity, as it does not require explicit channel estimation. The method capitalizes on DS spreading and interleaving across the carriers in a manner that allows for easy receive-side processing. We cast this method in a multi-channel receiver configuration (spatial diversity), and add frequency synchronization which operates jointly with data detection (equalization / despreading) using the principles described in [10]. To demonstrate the performance, we use experimental data recorded during the Mobile Acoustic Communications Experiment (MACE'10), adding varying amounts of noise to mimic the low SNR regime. Results are quite promising, showing satisfactory performance in sub-zero SNR conditions.

The rest of the paper is organized as follows. In Sec.II, we outline the basic principles of signal design and detection. Sec.III contains the results of experimental signal processing. We conclude in Sec.IV.

II. Signal Design and Detection

We consider an OFDM system with K carriers spanning bandwidth B. The carrier separation $\Delta f = B/K$ is chosen sufficiently narrow that the channel appears frequency-nonselective in each subband, yet wide enough that the channel remains approximately constant over each OFDM block of duration $T = 1/\Delta f$. In other words, we consider a properly designed OFDM system in which there is no ICI. The assumption of time-invariance does not include motion-induced frequency shifting, i.e. it refers to the channel after frequency synchronization. Additionally, the guard time between the blocks (cyclic prefix) is sufficiently long that multipath does not cause any inter-block interference.

With these notions, common to a conventional OFDM system design, the signals obtained after FFT demodulation can be modeled as

$$y_k = a_k H_k + z_k, k = 0, 1, \dots K-1 \tag{1}$$

where a_k is the symbol transmitted on the k-th carrier, $H_k = H(f_k)$ is the channel transfer function evaluated at the corresponding frequency $f_k = f_0 + k\Delta f$, and z_k is the noise. The noise is zero-mean, possibly uncorrelated across carriers.

The transmitted symbols a_k are obtained by coding (spreading) the original stream of information-bearing data symbols from a PSK (or QAM) alphabet. The length of the spreading sequence is chosen as $Q \geq BT_{mp}$, where T_{mp} is the multipath spread of the channel. This choice leads to a simple and elegant technique for channel estimation, as we will see later. Both K and Q are chosen as powers of 2 for ease of FFT processing. The spreading sequence can be a binary flip-coin random sequence, a maximum-length shift register sequence, or a custom-designed sequence such as Walsh-Hadamard, Gold or Kasami sequence. If noise protection only is sought on a point-to-point link, the choice of sequence is irrelevant. In multi-user applications, where interference is generated by other users of the same system, care has to be taken in assigning different sequences to different users.

The encoding process begins with mapping of each information-bearing data symbol onto a sequence of Q chips. With K carriers, $I = K/Q$ data symbols will form one OFDM block. Each symbol can have the same spreading code, or a different code, depending upon the desired level of security. So long as the code is known to the intended receiver, the conceptual system design does not change. Here, we will focus on using the same code for all the data symbols.

Denoting by d_i the $i-th$ data symbol, and by c_q the chips of the spreading sequence, the resulting sequence $d_0c_0, \dots d_0c_{Q-1}; d_1c_0, \dots d_1c_{Q-1}; \dots ; d_{I-1}c_0, \dots d_{I-1}c_{Q-1}$ is interleaved. Interleaving is employed to ensure that a given data symbol is spread evenly across the carriers, thus providing frequency diversity and ease of channel estimation on the receiver side. Specifically, the interleaved sequence yields data-modulated chips $a_k, \; k = 0, \dots K$, where $a_{qI+i} = d_i c_q$ $(q = 0, \dots Q-1; i = 0, \dots I-1)$. The data-modulated chips are assigned to consecutive carriers and transmitted. At the receiver, FFT demodulation yields the noisy observations (1).

A. Signal Detection

FFT demodulation is followed by the first stage of despreading. The known spreading sequence c_q is used to counter-multiply the observations y_k, yielding a new set of observations

$$x_{qI+i} = c_q^* y_{qI+i} = d_i H_{qI+i} + c_q^* z_{qI+i} \tag{2}$$

The newly formed observations are now arranged into I separate vectors (each of length Q),

$$\mathbf{x}_i = d_i \mathbf{H}_i + \mathbf{z}_i \tag{3}$$

where $\mathbf{H}_i = [H_i \; H_{i+\mathrm{I}} \; H_{i+2\mathrm{I}} \dots]^T$ is the relevant channel vector, and $\mathbf{z}_i$ the corresponding noise.

As in any OFDM system, post-FFT signal processing capitalizes on the discrete Fourier transform (DFT) model, by which the K frequency-domain channel coefficients $\{H_k\}$ are related to a set of delay-domain coefficients $\{h_l\}$. Because the OFDM block duration is (much) longer than the multipath spread of the channel T_{mp}, the number of significant coefficients h_l is (much) smaller than K.

Grouping the frequency-domain channel coefficients into a $K \times 1$ vector $\mathbf{H}$, and the significant delay-domain coefficients into an $L \times 1$ vector $\mathbf{h}$, the DFT relationship is stated as

$$\mathbf{H} = \mathbf{F}\mathbf{h} \tag{4}$$

where the $K \times L$ tall matrix $\mathbf{F}$ contains the first L columns of a regular $K \times K$ DFT matrix with elements $e^{-j2\pi kl/K}, \; k = 0, \dots K-1; \; l = 0, \dots L-1$.

Referring to the expression (3), we now have that

$$\mathbf{H}_i = \mathbf{F}_i \mathbf{h}, \; i = 0, \dots I-1 \tag{5}$$

where $\mathbf{F}_i$ is a $Q \times L$ matrix obtained from $\mathbf{F}$ by taking every I-th row, starting with row i. Consequently, the signals $\mathbf{x}_i$ can be expressed as

$$\mathbf{x}_i = d_i \mathbf{F}_i \mathbf{h} + \mathbf{z}_i \tag{6}$$

Multiplying the above expression by the conjugate-transpose $\mathbf{F}_i'$, and recognizing that $\mathbf{F}_i'\mathbf{F}_i = Q\mathbf{I}$,[1] we arrive at a new set of signals

$$\mathbf{u}_i = \frac{1}{Q}\mathbf{F}_i'\mathbf{x}_i = d_i\mathbf{h} + \mathbf{w}_i \tag{7}$$

The signals $\mathbf{u}_i$ serve as a starting point for detecting the data symbols d_i, $i = 0, \ldots I-1$. Two facts are worth noting at this point: (1) each of the signals $\mathbf{u}_i$ carries information about the respective data symbol d_i, but depends on the *same* channel vector $\mathbf{h}$, and (2) if the noise vectors $\mathbf{z}_i$ are uncorrelated (which typically is the case), so are the noise vectors $\mathbf{w}_i$. In addition, it is worth pointing out that if $\mathbf{h}$ is sparse, i.e. has fewer than L significant coefficients, additional reduction in dimensionality can be performed at this stage.

The data detection problem can now be stated as follows: given the observations $\mathbf{u}_i$, determine the symbols d_i from a given alphabet (e.g. QPSK).

If the channel vector were known, optimal data detection would be performed by making a soft estimate $\hat{d}_i = \mathbf{h}'\mathbf{u}_i/||\mathbf{h}||^2$, and using it to make the decision $\tilde{d}_i = \text{dec}\ (\hat{d}_i)$. Additional channel coding, if applied, can be exploited at this point as well.

In practice, of course, the channel is not known, and an estimate $\hat{\mathbf{h}}$ has to be used instead of $\mathbf{h}$. Below, we propose two approaches for dealing with the unknown channel, one based on coherent detection using channel estimation, and the other based on differentially coherent detection.

1) Coherent detection: Assigning one of the data symbols as a pilot in an OFDM block, say d_0, the channel can be estimated as

$$\hat{\mathbf{h}} = \hat{\mathbf{h}}_0 = d_0^*\mathbf{u}_0 \tag{8}$$

This channel estimate can now be used to estimate the remaining data symbols as

$$\hat{d}_i = \hat{\mathbf{h}}'\mathbf{u}_i/||\hat{\mathbf{h}}||^2, \ i = 1, \ldots I-1 \tag{9}$$

Data detection follows through decision-making,

$$\tilde{d}_i = \text{dec}\ (\hat{d}_i) \tag{10}$$

While this is the basic principle of coherent detection, an alternative method can be used to improve the performance. Namely, after making the first tentative decision $\tilde{d}_1$, the corresponding channel estimate is formed as

$$\hat{\mathbf{h}}_1 = \tilde{d}_1^*\mathbf{u}_1 \tag{11}$$

This instant estimate is used to form a running average

$$\hat{\mathbf{h}} = \frac{1}{2}(\hat{\mathbf{h}}_0 + \hat{\mathbf{h}}_1) \tag{12}$$

which is set as the current channel estimate, and used to make the next symbol decision. The procedure continues until the last symbol decision has been made. With the final channel estimate $\mathbf{h}$, a fresh set of all symbol decisions is made according to (9), (10).

Note that the data estimation step (9) effectively accomplishes a second stage of despreading, whereby the multipath components are combined, i.e. their contributions are summed in a coherent manner. Refinements to the above procedure are also possible, including joint data detection and channel estimation, as well as the use of dedicated sparse channel estimation techniques. Coherent detection can further be improved by engaging a decision-directed mode of operation.

2) Differentially coherent detection: Our first stage of processing, which yields the signals $\mathbf{u}_i$ given by the expression (7), can be followed by differentially coherent detection, which eliminates the need for explicit channel estimation. Differentially coherent detection of OFDM signals has been analyzed within a standard (non-spread) system framework, showing excellent performance results in tests with real data [9], [10]. This fact serves as a motivation to investigate its use in the present DS OFDM setting.

Differentially coherent detection makes use of differential encoding performed at the transmitter, whereby the transmitted data symbols d_i are formed from the original information-bearing symbols b_i as $d_i = b_i d_{i-1}$. In doing so, the first data symbol d_0 is set to a known value, e.g. 1. Note that differential encoding is performed in the frequency domain (across carriers), not in the time domain.

Differentially coherent detection is now accomplished simply by forming the estimates

$$\hat{b}_i = \mathbf{u}_{i-1}'\mathbf{u}_i/||\mathbf{u}_{i-1}||^2 \tag{13}$$

and making the corresponding decisions $\tilde{b}_i = \text{dec}\ (\hat{b}_i)$.[2] The obvious advantage of differentially coherent detection is its simplicity of implementation. There is no need for explicit channel estimation, and all post-FFT processing is reduced to inner product operations.

The system architecture, including transmitter and the various approaches to detection, is illustrated in Fig.1.

B. Multi-channel processing

On the receiver side, extension to spatial diversity reception follows the principles of maximum-ratio combining (MRC) for coherent detection, or differential maximum-ratio combining (DMRC) for differentially coherent detection. Both extensions are straightforward.

Assuming M receiving elements, their FFT outputs $\mathbf{y}^m, m = 1, \ldots M$, are fed into M identical processors, which produce the observations

$$\mathbf{u}_i^m = d_i\mathbf{h}^m + \mathbf{z}_i^m \tag{14}$$

Assuming independent, identically distributed noise components, MRC yields the decision variables

$$\hat{d}_i = \frac{1}{\sum_{m=1}^M ||\hat{\mathbf{h}}^m||^2}\hat{\mathbf{h}}^{m'}\mathbf{u}_i \tag{15}$$

[1]Recall that $Q \geq L$.

[2]Normalization can be omitted with PSK, both in coherent and differentially coherent detection.

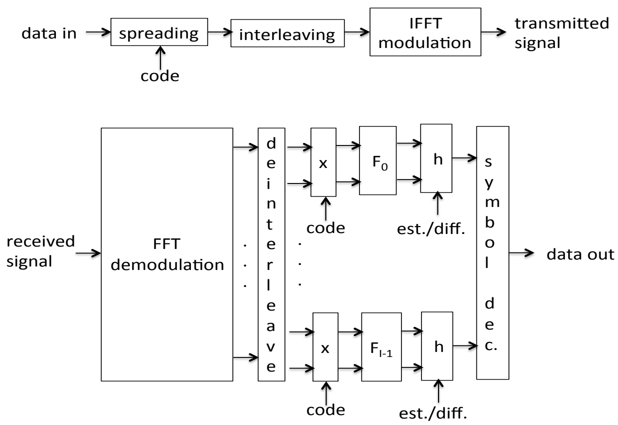

Fig. 1. Block diagram of the transmitter / receiver architecture. The length of the spreading code Q and the number of carriers K correspond to $I = K/Q$ data symbols comprising one OFDM block. Channel estimation can be performed explicitly, leading to coherent detection. Alternatively, differentially coherent detection can be used. In either case, frequency-domain channel equalization is represented by the blocks following the spreading code removal (total of I such blocks). This figure illustrates a single-input single-output system architecture, which serves as a basis for a multi-channel architecture.

Analogously, DMRC yields

$$\hat{b}_i = \frac{1}{\sum_{m=1}^{M} ||\mathbf{u}_{i-1}^m||^2} \mathbf{u}_{i-1}^{m'} \mathbf{u}_i \tag{16}$$

Again, normalizing the magnitude of the data estimate is significant only if any subsequent adaptive processing is driven by the data estimation error $e_i = \hat{d}_i - d_i$ (e.g., block-by-block adaptive channel estimation); otherwise, it can be omitted for PSK symbols.

C. Frequency offset compensation

So far, we have assumed that the channel is time-invariant over one OFDM block. This assumption is contingent upon accurate frequency synchronization. If the received signal contains a frequency offset, which typically is the case due to the Doppler effect, proper correction has to be made.

Denoting by $v_m(t)$ the m-th element's received signal down-shifted by the lowest carrier frequency f_0, and by $\hat{\beta}$ an estimate of the radial frequency shift, the post-FFT signal is given by

$$y_k^m = \int_T v_m(t) e^{-j\hat{\beta}t} e^{-j2\pi k\Delta f t} dt \tag{17}$$

If synchronization is accurate, the model (1) will hold, and our approach to data detection will be justified. Otherwise, a residual frequency shift will cause ICI, invalidating our model and disturbing the detection process. The data symbol estimate (15) will thus depend on the value $\hat{\beta}$, and so will the corresponding squared error

$$E_d(\hat{\beta}) = \sum_i |\hat{d}_k(\hat{\beta}) - \tilde{d}_k(\hat{\beta})|^2 \tag{18}$$

The same will be true for differential detection (16), where

$$E_b(\hat{\beta}) = \sum_i |\hat{b}_k(\hat{\beta}) - \tilde{b}_k(\hat{\beta})|^2 \tag{19}$$

Following the approach of [10], we calculate the squared error for a number of hypothesized values $\hat{\beta}$, and chose the best hypothesis as

$$\tilde{\beta} = \arg\min_{\hat{\beta}} E_d(\hat{\beta}) \tag{20}$$

The final symbol decisions are $\tilde{d}_i(\tilde{\beta})$. Identical procedure is used for differentially coherent detection.

Hypothesis testing can be used alone, or it can be augmented by a stochastic gradient approach for estimating the frequency offset in a closed-loop manner. The stochastic gradient approach provides additional accuracy and speeds up the computation. Description of this algorithm is lengthy; suffice it to say that it closely follows the approach of [10].

III. Experimental Results

The Mobile Acoustic Communications Experiment (MACE'10) was conducted in June 2010 off the coast of Martha's Vineyard island in the North Atlantic. A vertical array with 12 elements separated by 12 cm received the signals transmitted from a source moving to-and-from the receiver at a varying speed of up to 1.5 m/s. The system was deployed mid-column in about 100 m of water, while transmission distance varied between 3 km and 7 km. Acoustic signals were transmitted in the 10.5 kHz - 15.5 kHz band. A total of 52 transmissions were made over a period of 3.5 hours. Each transmission contained a suite of OFDM signals with varying number of carriers. The signal parameters are summarized in Table III.

TABLE I
Signal Parameters

bandwidth, B	5 kHz
lowest carrier frequency, f_0	10.5 kHz
guard time, T_g	16 ms

number of carriers, K	128	256	512	1024	2048
OFDM blocks per frame	64	32	16	8	4
carrier spacing [Hz]	39.1	19.5	9.8	4.9	2.4
chip rate, $\frac{B}{1+BT_g/K}$ [kbps]	3.0	3.8	4.3	4.6	4.8

We present the results of QPSK data detection, measuring the performance in terms of the mean squared error (MSE) and symbol error rate (SER). The results shown here represent the average taken over the 52 transmissions.

In estimating the frequency offset, the range of hypothesized values $\hat{\beta}/2\pi$ is set to $\pm 3\Delta f$, with resolution $\Delta f/10$. A full search is performed only in the first OFDM block of a frame; from there on, the range of hypothesized values can be narrowed around the existing estimate, or stochastic gradient search can be used.

Fig.2 (top) shows the estimated MSE obtained after processing the MACE signals with varying number of carriers ranging from $K = 128$ to 2048. All $M = 12$ receiving elements are used for combining. Results are shown for coherent and differentially coherent detection, with varying processing gain Q. Unstructured, binary flip-coin spreading sequences are used. The MSE is calculated as the average over $I-1$ data symbols in an OFDM block (the remaining symbol is the pilot), and all blocks of the 52 transmissions. The performance clearly improves with the processing gain Q. The amount of improvement is generally about 3 dB for every doubling of Q; an occasional deviation at lower values of Q likely occurs because the assumption $Q \geq BT_{mp}$ is only partly satisfied. The MSE generally decreases as the number of carrier grows, but reaches a turning point at $K = 1024$ as the time-coherence assumption weakens. This trend has been observed previously as well [9], [10]. Coherent detection generally outperforms differential detection by about 6 dB-8 dB. This gain is a result of averaging the channel estimate over $I = K/Q$ symbols (and is again contingent upon the assumption $Q \geq BT_{mp}$ being satisfied).

Fig.2 (bottom) shows the estimated MSE vs. the number of receiving elements M. The number of carriers is $K = 1024$ in this example. The receiving elements are chosen among the 12 available as equally spaced whenever possible ($M = 2, 3, 4, 6$). As expected, the performance improves as the array size grows, but exhibits the effect of diminishing returns due to the finite aperture (the elements become more closely spaced as their number grows, thus introducing correlation). The strikingly good performance comes at the price of a Q-fold reduction in bit rate, $R_b = \frac{1}{Q} \cdot \frac{2B}{1+T_g B/K}$.

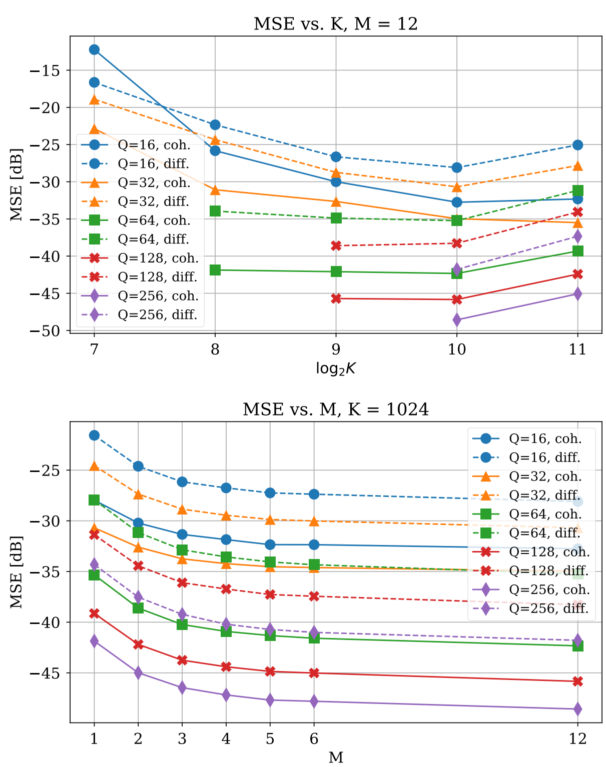

Fig. 2. Estimated mean squared error: average over 52 MACE transmissions.

Results of Fig.2 were obtained to calibrate the system with raw received signals that were not altered to contain more noise than they naturally did. To assess the system performance in low SNR conditions, noise was added artificially to the recorded signals. To do so, noise-only recordings were used to extract the noise statistics first. Specifically, the noise components z_k^m that contaminate the post-FFT observations (1) were modeled as zero-mean Gaussian, uncorrelated across the carriers (k), but correlated across the receiving elements (m). The spatial correlation matrix was estimated from the recordings, and used to generate samples of the spatially-colored noise from computer-generated independent Gaussian samples. The results are shown in Figs.3 and 4. As a benchmark, these results include the spatially-white noise case. The difference in performance observed with colored / white noise reinforces the need to have sufficient separation between the array elements.

Fig.3 shows the performance of coherent detection, while Fig.4 refers to differentially coherent detection. The symbol error rate refers to uncoded QPSK symbols; additional channel coding can of course be applied to further improve the SER. Both sets of results (coherent and differential) exhibit the same trend. The MSE "saturation" beyond 20 dB of SNR is an artifact of adding noise to an already noisy signals. Namely, the SNR value used to label the figures refers to the artificial noise only. As this noise vanishes, the actual SNR does not tend to zero, but instead remains at the level already present in the raw recorded signals. Coherent detection outperforms differential detection when $Q > 32$; however, one must note that differential detection still offers excellent performance, while its computational cost is minimal.

The results of Figs.3 and 4 can be used as a guideline for designing a multi-carrier system that needs to operate in low SNR. To do so, one would set a bar on the MSE, say -10 dB (this bar corresponds to a certain SER with or without channel coding), and look for those K, Q pairs that meet the bar. For example, if the system were to be deployed in the MACE environment, and required to operate at the SNR of -10 dB, we see that the processing gain needed with $K = 1024$ carriers is $Q = 64$ or more. Assuming a guard interval $T_g = Q/B$, the resulting bandwidth efficiency is $\frac{1}{Q} \cdot \frac{1}{1+Q/K}$ symbols per second per Hz of occupied bandwidth. With QPSK modulation, 1024 carriers, processing gain of 64 and 5 kHz of bandwidth, the resulting bit rate is 147 bps. Hopefully, an application that requires operation in -10 dB of SNR, will find this bit rate to be sufficient.

IV. Conclusion

We addressed the problem of acoustic signal detection in low SNR conditions by proposing a multi-carrier modulation method integrated with direct-sequence spectrum spreading. The method capitalizes on structured coding across the carriers, enabling a de-facto despreading operation to reveal the channel in the impulse response domain. Following this operation, either coherent or differentially coherent detection can be applied towards extracting the multipath gain. Detection is integrated with a custom-designed frequency offset estimation technique, which is necessary for a practical application to mobile acoustic systems.

Results of processing an experimental data set recorded over a mobile acoustic channel with externally added Gaussian noise clearly demonstrate successful operation in sub-zero SNR conditions. Such operation owes to three key factors: accurate frequency synchronization, multi-channel diversity

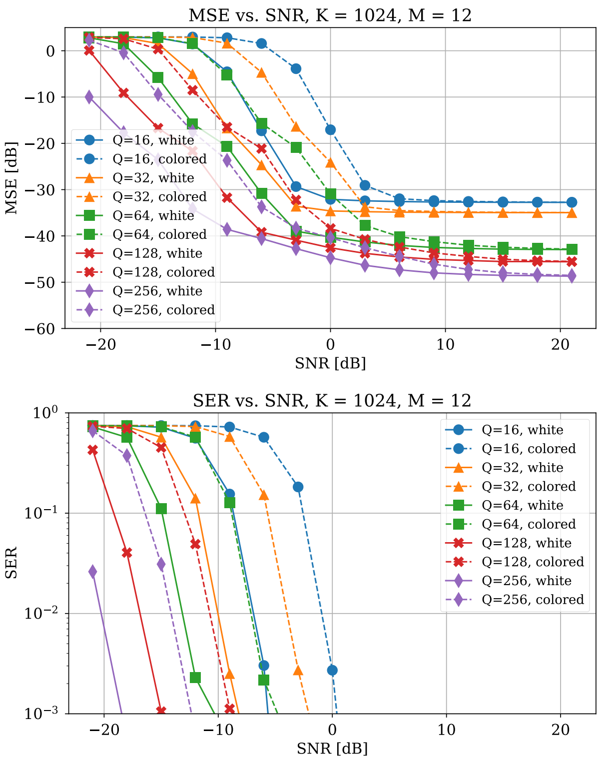

Fig. 3. Mean squared error and symbol error rate obtained with coherent detection. $K = 1024$ carriers, $M = 12$ receiving elements. The SNR refers to the artificially added noise (as artificial noise vanishes, natural noise remains, hence the MSE reaches a plateau).

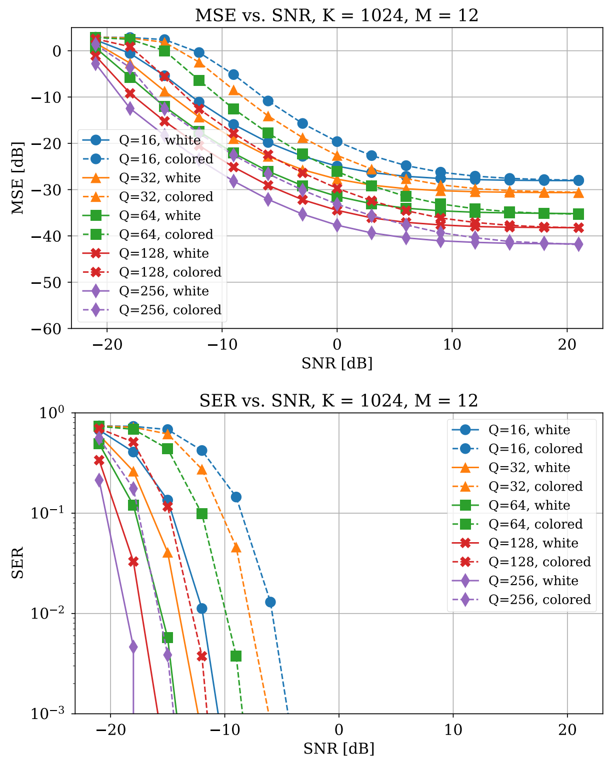

Fig. 4. Mean squared error and symbol error rate obtained with differentially coherent detection. $K = 1024$ carriers, $M = 12$ receiving elements. The SNR refers to the artificially added noise (as artificial noise vanishes, natural noise remains, hence the MSE reaches a plateau).

reception, and the proposed structure of despreading/multipath processing. While coherent detection outperforms differential detection, the latter nonetheless offers very good performance without explicit channel estimation, i.e. at a very low computational complexity.

Future research will focus on several aspects: (1) integration of super-resolution and sparse channel estimation methods into coherent detection, (2) time-adaptive receiver operation, and (3) multi-carrier CDMA networks. The latter is notably motivated by the present results, as multi-carrier multi-user interference exhibits Gaussian-like characteristics, for which the present system was shown to be well suited.

References

[1] M.Stojanovic and L.Freitag, "Multi-channel detection for wideband underwater acoustic CDMA communications," *IEEE J. Oceanic Eng.*, vol.31, No.3, July 2006, pp.685-695.

[2] C.He, J.Huang and Z.Ding, "A variable-rate spread-spectrum system for underwater acoustic communications," *IEEE J. Oceanic Eng.*, vol.34, No.4, Oct. 2009, pp.624-633.

[3] J.Ling, H.He, J.Li, W.Roberts and P.Stoica, "Covert underwater acoustic communications," *J. Acoust. Soc Am.*, vol.128, No.5, 2010, pp.2898-909.

[4] F.Qu, X.Qu, L.Yang and T.C.Yang, "Spread-spectrum method using multiple sequences for underwater acoustic communications," *IEEE J. Oceanic Eng.*, vol.43, No.4, Oct. 2018, pp.1215-1226.

[5] S. Liu, G. Qiao, and A. Ismail, ?Covert underwater acoustic communication using dolphin sounds,? *J. Acoust. Soc Am.*, vol.133, No.4, 2013, pp.300?306,

[6] D.Kalofonos, M.Stojanovic and J.Proakis, "Performance of Adaptive MC-CDMA Detectors in Rapidly Fading Rayleigh Channels," *IEEE Trans. Wireless Commun.*, vol.2, No.2, March 2003, pp.229-239.

[7] G G.Leus and P. van Walree, "Multiband OFDM for covert acoustic communications," *IEEE J. Select Areas Commun.*, vol.26, No.4, Dec. 2008, pp.1662-1673.

[8] C.Berger, S.Zhou, J.Preisig and P.Willet, "Sparse channel estimation for multi-carrier underwater acoustic communication: from subspace methods to compressed sensing," I*EEE Trans. Sig. Proc.*, vol.58, No.3, March 2010, pp. 1708-1721.

[9] Y.Aval and M.Stojanovic, "Differentially coherent multi-channel detection of Acoustic OFDM signals," *IEEE J. Oceanic Eng.*, vol.40, No.2, April 2015, pp.251-268.

[10] A.Tadayon and M.Stojanovic, "Low-complexity super-resolution frequency offset estimation for high data rate acoustic OFDM systems," *IEEE J. Oceanic Eng.*, Sept. 2018, DOI:10.1109/JOE.2018.2869657.